Role of Transferred Static Stress Due to Sarpol-e Zahab Earthquake in Aftershock Distribution

Behnam Maleki Asayesh[1], Hamid Zafarani[2*], and Neda Najafi[2]

1. Ph.D. Student, International Institute of Earthquake Engineering and Seismology (IIEES), Tehran, Iran
2. Associate Professor, Seismological Research Center, International Institute of Earthquake Engineering and Seismology (IIEES), Tehran, Iran,
* Corresponding Author; email: h.zafarani@iiees.ac.ir
3. M.Sc. Student, International Institute of Earthquake Engineering and Seismology (IIEES), Tehran, Iran

Received: 18/08/2018
Accepted: 10/10/2018

ABSTRACT

By using slip model from USGS and focal mechanism and aftershocks distribution from Iranian Seismological Center (IRSC) for Sarpol-e Zahab earthquake (Mw 7.3) on November 12, 2017, we investigated the correlation between Coulomb stress changes and aftershocks distribution. In this study, about 500 aftershocks with magnitude larger than 2.5 and azimuthal gap less than 180 degrees were selected. Calculated Coulomb stress changes on the optimally oriented faults showed that most of the seismicity occurred in regions of increased stress and the majority of them concentrated on the ruptured plane, especially in west and south parts. Besides, nodal planes of the selected 11 aftershocks received positive Coulomb stress changes. Therefore, there is a good correlation between Coulomb stress changes and aftershocks distribution in Sarpol-e Zahab event. Furthermore, calculated static stress on the surrounding faults showed that middle part of the High Zagros Fault (HZF), the northern part of the Main Recent Fault (MRF), and the northern part of the Zagros Foredeep Fault (ZFF) are located in the positive stress change area.

Keywords:
Sarpol-e Zahab earthquake; Coulomb stress changes; Aftershocks; West of Iran

1. Introduction

The active tectonics of Iran is dominated by the convergence of Arabian and Eurasian plates. Approximately 22 mm/year of this convergence, is accommodated through crustal shortening and thickening by the Zagros Thrust Zone and a part of that is transferred to the Alborz and Kopet Dagh Thrust Zones in the Northern Iran [1]. The November 12, 2017 Sarpol-e Zahab earthquake occurred along the northwestern part of the Zagros Thrust Zone near the political boundary between Iraq and Iran and caused hundreds of deaths and thousands of injuries and building damages and collapses, especially in Kermanshah province of Iran. The epicenter location of the event suggests that the NNW trending Mountain Front Fault (MFF) has been responsible for the earthquake though it was not associated with surface faulting.

The permanent deformation of the surrounding crust is the consequence of an earthquake fault rupture. This earthquake changes the stress on nearby faults as a function of their locations; geometry and sense of slip (rake) [2]. This kind of static stress changes are small but permanent and helps determine the location of the future earthquakes although it cannot provide good estimate of the time of the next events [3]. Recently, many seismologists

worldwide have focused on this issue and the correlation between the mainshock and subsequent aftershocks in an earthquake sequence. Many studies on large earthquake sequences have concluded that stress changes from the mainshock affect the locations of subsequent aftershocks [4-5]. The coulomb stress triggering theory has been proposed for evaluating aftershock hazards after great earthquakes. This theory implies that aftershocks and subsequent mainshocks often occur in regions that experienced an increase in Coulomb stress caused by the mainshock, and earthquakes become less prevalent than before the mainshock in regions subject to a Coulomb stress drop. It was thought that small Coulomb stress changes can alter the likelihood of earthquakes on nearby faults [6-8]. The objective of this study is to calculate the Coulomb stress changes due to the Sarpol-e Zahab earthquake on the optimally oriented thrust faults and nodal planes of some aftershocks for investigating the correlation between Coulomb stress changes and aftershocks distribution. The Coulomb stress changes on the surrounding faults has also been calculated.

2. Study Region

The active tectonic environment in Iran is related to the convergence of the Eurasian and Arabian plates [9]. The continental collision along the Zagros suture resulted from the long-lasting convergence of these two plates and has provided the essential force raising the Zagros Mountains and uplifting the Iranian plateau. The collision was initiated at ~35 Ma and continued to the final stage at ~12 Ma [10]. The main Zagros reverse fault (MZRF) and the main recent fault (MRF) in the south and north Zagros, respectively are the major faults in Zagros [1]. Based on Motaghi et al. [11] study, crustal thickness beneath Zagros increases gently from 43 to 59 km beneath MRF and there is an intracontinent low-strength shear zone between Arabia and Central Iran. Shortening and earthquake deformation within Iran is mainly accommodated by faults in the Zagros, Alborz, Kopet Dagh, and west of the Dasht-e Lut [9]. The high level of seismicity observed in the Zagros indicates the accommodation of ongoing deformation partly through seismic activity in the belt. The seismic moment release mostly occurs in the SW topographic edge of the belt [12].

At 21:48' (local time), on November 12, 2017, a strong quake of magnitude 7.3 struck the region west of Kermanshah city (within Zagros structural domain), in western Iran. The parameters of this event based on different references are summarized in Table (1). Solaymani Azad et al. [13] undertook InSAR imagery and interferometry analysis and active tectonic field studies to assess the causative fault and the probable co-seismic surface faulting. Their preliminary assessment highlighted the concentration of the secondary order co-seismic geological features on the hanging wall of the mountain front fault (MFF), close to the high Zagros fault (HZF) zone.

Following the Sarpol-e Zahab event (Mw 7.3) about 500 aftershocks (Mn ~2.5 and azimuthal gap less than 180 degrees) have been recorded by permanent networks of the Iranian Seismological Center (IRSC) at the Institute of Geophysics of Tehran University during 6 months (Figure 1). These aftershocks are reliable in latitude and longitude (epicenter). Majority of these aftershocks are focused in the west and south part of the ruptured fault plane in the direction of the rake orientation. Among these aftershocks, there are 11 events that their focal mechanisms have been solved by Iranian Seismological Center (IRSC). These events are shown in Figure (2) and their parameters are summarized in Table (2).

3. The Coulomb stress triggering hypothesis

Earthquakes occur when the stress exceeds the strength of the rocks along the fault [15]. The closeness to failure of a fault is computed using the changes in the Coulomb failure function (ΔCFF), which is the Coulomb stress changes, depend on both

Table 1. Parameters of the Sarpol-e Zahab earthquake. Location is from IRSC and fault parameters are from USGS.

Lat. (°)	Lon. (°)	Depth (km)	Length (km)	Width (km)	Moment ($*10^{27}$) dyne.cm	Strike (°)	Dip (°)	Rake (°)
34.77	45.76	18	85	72	1.2	352	16	138

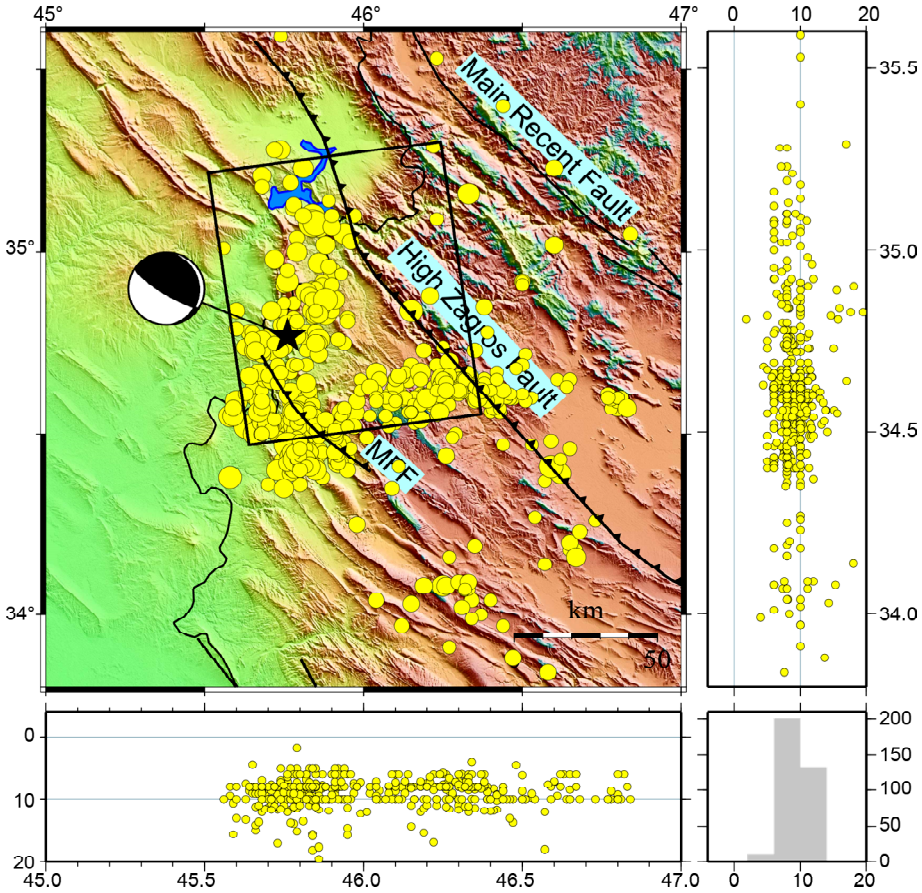

Figure 1. Main tectonic features of the study area. Location (black star from IRSC) and focal mechanism of the Sarpol-e Zahab earthquake (from USGS) with the epicenter of about 500 aftershocks (yellow circles) from IRSC are shown. Faults are from Hessami et al. [14]. The solid black rectangle shows the surface projection of slipped plane. MFF is Mountain Front Fault.

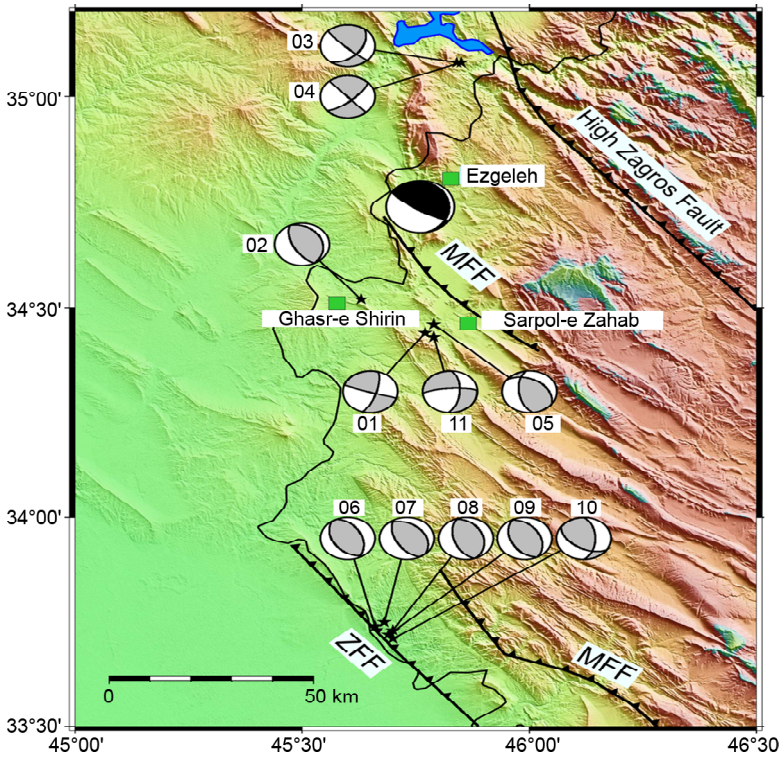

Figure 2. Focal mechanism of Sarpol-e Zahab earthquake (black and big beach ball) and its 11 aftershocks (gray and small beach balls). Focal mechanism of the mainshock is from USGS and focal mechanism of aftershocks are from IRSC. Green squares show the cities near the epicenter of the mainshock. Faults are from Hessami et al. [14]. MFF is Mountain Front Fault and ZFF is Zagros Foredeep Fault.

Table 2. Parameters of 11 aftershocks from Iranian Seismological Center. (N: number, d: date, h: hour, Lon: longitude, Lat: latitude, Dep: depth, Mw: moment magnitude, P: nodal plane, S: strike, D: dip, R: rake, and ΔCFF: Coulomb stress changes).

N	d	h	Lon.	Lat.	Dep.	Mw	P1				P2			
							S	D	R	ΔCFF	S	D	R	ΔCFF
01	17/11/13	09:19	45.77	34.44	08.3	4.4	017	72	178	0.645	108	88	018	-0.157
02	17/11/18	04:12	45.63	34.52	13.2	4.5	153	63	089	1.679	335	27	092	-1.050
03	17/12/11	14:09	45.84	35.08	08.0	5.4	134	83	042	2.910	038	49	171	2.485
04	17/12/11	14:42	45.85	35.08	06.0	4.6	048	72	179	3.836	138	89	018	2.930
05	18/01/08	15:22	45.79	34.46	08.0	5.0	172	59	119	1.002	305	42	051	-0.007
06	18/01/11	06:59	45.69	33.71	08.4	5.5	146	45	082	0.023	337	46	098	0.004
07	18/01/11	07:14	45.71	33.72	09.4	5.3	152	57	098	0.030	317	34	078	0.009
08	18/01/11	07:55	45.70	33.73	08.2	4.8	162	54	092	0.018	338	36	087	0.002
09	18/01/11	08:00	45.69	33.72	10.9	5.2	154	47	091	0.021	332	43	089	-0.001
10	18/01/19	22:17	45.70	33.71	08.8	4.9	123	52	047	0.021	000	55	131	0.024
11	18/04/01	08:35	45.79	34.43	07.3	5.0	266	77	-031	0.586	004	60	-164	0.990

changes in shear stress ($\Delta\tau$) that reckoned positive when sheared in the direction of fault slip and normal stress ($\Delta\sigma$) that is positive if the fault is unclamped, and defined as follows:

$$\Delta CFF = \Delta\tau + \mu'\Delta\sigma \quad (1)$$

where μ' is the apparent coefficient of friction which includes the unknown effect of pore pressure change as well [8]. Depending on pore fluid content of the fault zone, μ' changes between 0.2 and 0.8. Lower than 0.2 suggested for well-developed and repeatedly ruptured fault zones because on these zones sliding friction drops cause of trapped pore fluids. On the other hand, higher than 0.8 amount can be used for young minor faults, since they did not have enough displacement for trapping pore fluids [8, 15-18]. Positive ΔCFF promotes failure, and negative inhibit it [2]. The occurrence of earthquake activity can be promoted when the Coulomb stress increases as little as 0.1 bar on a seismogenic fault [8].

4. Coulomb Stress Changes on the Optimally Oriented Faults

Coulomb 3.4 software was used to calculate the co-seismic static stress changes due to the Sarpol-e Zahab earthquake on the optimally oriented faults. Moreover, the Earth was assumed as a homogeneous elastic half-space, and faults were considered as rectangular dislocations embedded within. In order to consider these assumptions in our calculation, Young modulus, shear modulus, Poisson ratio, and coefficient friction were considered equal to 8 × 105 bar, 3.2 × 105 bar, 0.25, and 0.4, respectively.

In addition to parameters describing fault geometry (e.g., location and dip angle) and elastic properties of the material, an estimate of the amount of slip on the fault and regional stress field is necessary to model the Coulomb stress changes on optimally oriented faults. Therefore, we need the slip model of the earthquake and regional (tectonic) stress. A more realistic finite fault failure model is critical for the following calculation of Coulomb stress changes. Here, a variable finite fault model was selected that was inverted from Global Seismic Network (GSN) broadband waveforms by USGS (Figure 3). In this model, the distribution of the amplitude and slip direction for subfault elements of the fault rupture model are determined by the

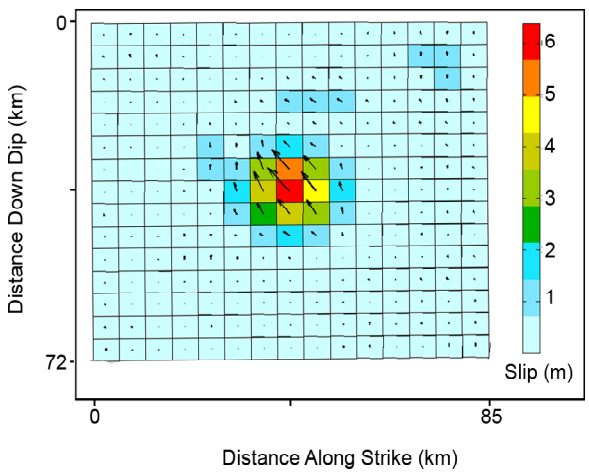

Figure 3. The finite fault model of the M 7.3 Sarpol-e Zahab earthquake. It is subdivided in 15 patches along the strike and 15 patches along the dip. The black arrows within each patch represent the slip direction. The bar on the right indicates the slip amount of each patch.

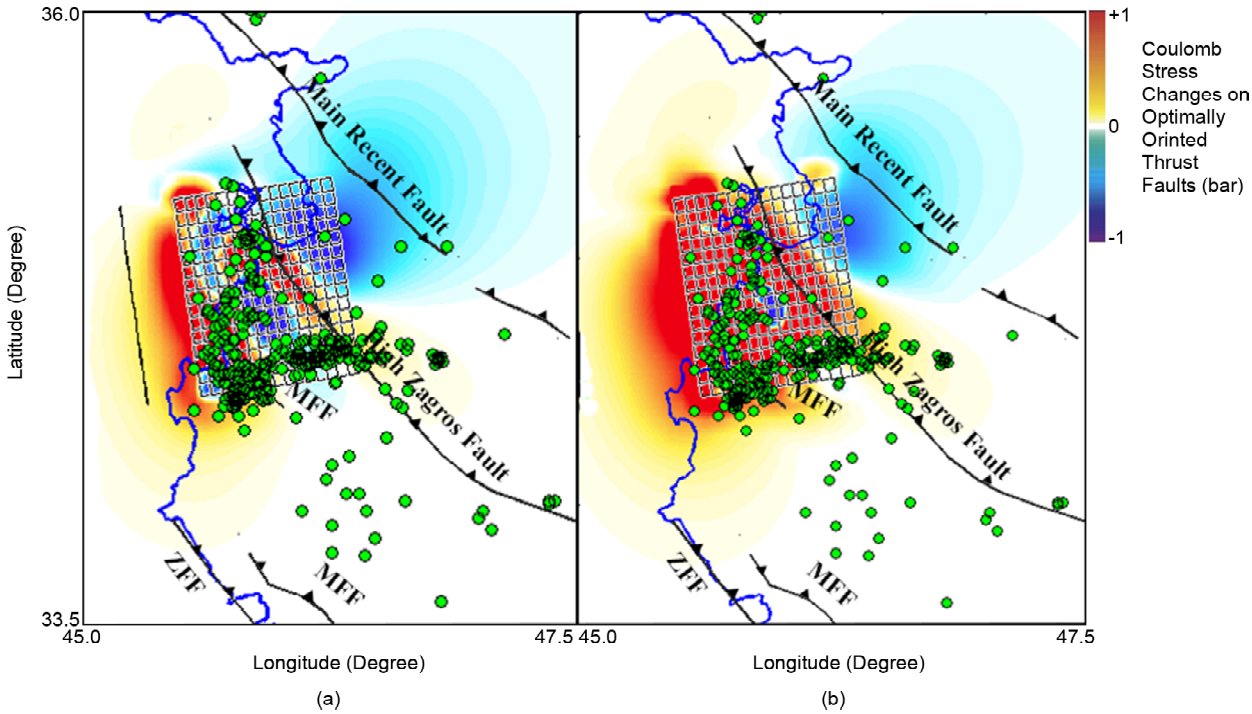

Figure 4. Coulomb stress changes and seismicity. a) Coulomb stress changes due to Sarpol-e Zahab earthquake on the optimally oriented thrust faults. The calculation had been computed in 7.5 km depth and aftershocks are shown with green circles. b) Maximum resolved stress changes on optimally oriented thrust faults due to Sarpol-e Zahab earthquake for the depth range of 0.0-20.0 km and distribution of aftershocks (green circles) that occurred until May 20, 2018 during about six months.

inversion of teleseismic body waveforms and long period surface waves.

As shown in Figure (3), the different colors indicate the slip amount. The deeper the color, the greater the amplitude of the slip. Arrows indicate the slip direction (of the hanging wall with respect to the foot wall). Based on focal mechanisms stress inversion, seismic strain rate, and geodetic strain rate weighted average azimuth of compression axis for this region is about 45.92 degree [19].

Coulomb stress changes due to this event on the optimally oriented thrust faults (Figure 4) were calculated, and it was observed that most of the seismicity occurred in the ruptured plane especially in the west and south edge where the stress changes are positive and imparted stress on the optimally oriented faults had been increased. Thus, there is a good correlation between Coulomb stress changes due to the Sarpol-e Zahab earthquake and the location of its aftershocks until May 20, 2018 during about six months. Figure (4a) shows imparted stress on the optimally oriented faults in the depth of 7.5 km. It is obvious that the seismicity is willing to distribute in the red area where the Coulomb stress changes are positive, and they are scarce in the blue area where the transferred stress is negative. We can see two trends of distributed aftershocks. An east-west oriented aftershock that completely located in the positive stress changes area and a north-south orientation that its trend changes as soon as receiving negative stress changes (blue area). Figure (4b) shows the maximum imparted stress on the optimally oriented faults for the depth range of 0.0-20.0 km.

5. Coulomb Stress Changes Computed on Nodal Planes

If focal mechanism information is available, we can test whether the fault plane associated with each earthquake was brought closer to failure or not, and this is presumably a more stringent test than determining if earthquakes occurred in the red regions. Imparted Coulomb stress changes that resolved on the nodal planes of the aftershocks of the Sarpol-e Zahab earthquake were calculated to examine that they were brought closer to failure or not.

For this purpose, 11 aftershocks with available focal mechanisms from Iranian Seismological Center (IRSC) were used. Parameters of these

events are summarized in Table (2) and shown in Figure (2) with their numbers. We calculated Coulomb stress changes due to the Sarpol-e Zahab earthquake on the nodal planes of these aftershocks. The calculation showed that the first nodal plane of these events received positive stress changes. Events number 03 and 04 that located in the north part of the ruptured fault plane of the mainshock received a large amount of stress changes on both nodal planes. All events that located in the southwest of the ruptured plane of the mainshock (number 01, 02, 05, and 11) received positive stress changes on the first nodal plane. Only event number 11 received positive stress changes on the second nodal plane and three others received negative stress changes on their second nodal planes (Figure 2 and Table 2).

All aftershocks that located in the south (number 06, 07, 08, 09, and 10) on the Zagros Foredeep Fault (ZFF) received positive stress changes and only number 09 event received negative stress changes on the second nodal plane that is negligible. Imparted stress on nodal planes of these aftershocks are small because of the far distance but it seems to be enough to trigger them on the ZFF (Figure 2 and Table 2). In summary, it is obvious that transferred Coulomb stress changes on the nodal planes of aftershocks triggered them that is a good evidence for the correlation between transferred stress and distribution of aftershocks.

6. Coulomb Stress Changes on the Surrounding Faults

The Coulomb stress changes due to Sarpol-e Zahab earthquake on the surrounding faults were calculated in order to know whether they are brought closer to rupture or not. Reverse faults with northwest-southeast direction were considered as receiver faults. The calculation indicated that the middle part of the high Zagros fault (HZF) and the northern part of the main recent fault (MRF) and Zagros foredeep fault (ZFF) are located in the positive stress change area (Figure 5). It should be considered that above-mentioned aftershocks that occurred on the ZFF are located in the place where stress changes are positive. These area with positive Coulomb stress changes can be the location of the future large earthquakes. In other words, probability

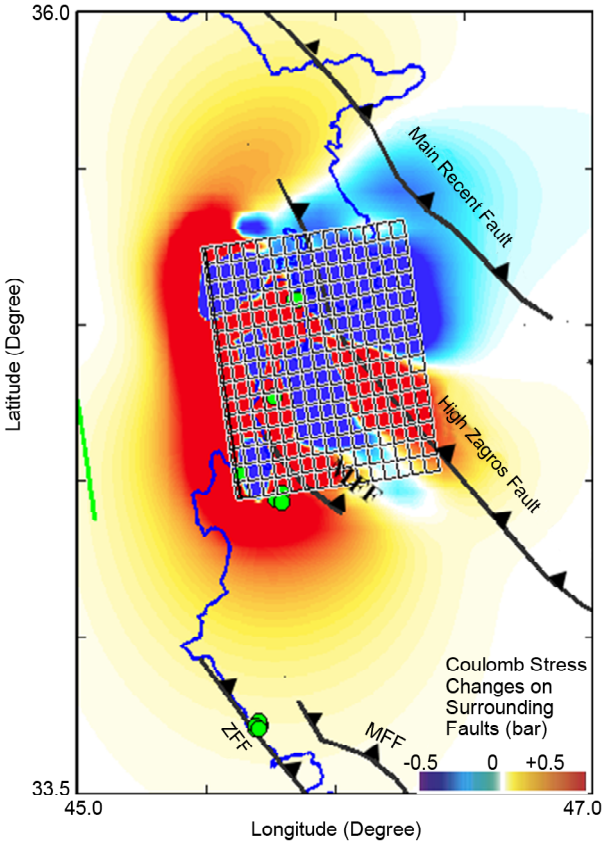

Figure 5. Coulomb stress changes due to the Sarpol-e Zahab earthquake on the surrounding reverse faults. The calculation had been computed in 15 km depth. Location of the above-mentioned aftershocks is shown with green circles.

of the future events are high in these parts of the faults.

7. Conclusion

In order to investigate a probable correlation between Sarpol-e Zahab earthquake and seismicity, about 500 aftershocks (Mn $\geq$ 2.5 and azimuthal gap less than 180 degrees) were used during six months. For this purpose, the variable-slip model of Sarpol-e Zahab earthquake (Figure 3) was used. Our computation revealed that most of the seismicity occurred in the ruptured plane especially its south edge where the stress changes are positive and imparted stress on the optimally oriented faults had been increased and few of them located in the places that Coulomb stress changes are negative (Figure 3). Imparted stress on the nodal planes of the 11 selected aftershocks indicates that they received positive stress changes at least in one nodal plane. This can be an evidence for the correlation between transferred stress and seismicity. Transferred stress on the surrounding faults

showed that the middle part of the high Zagros fault (HZF), the northern part of the main recent fault (MRF), and the northern part of the Zagros foredeep fault (ZFF) received positive stress changes.

As a result, aftershock locations of the Sarpol-e Zahab earthquake, correlate well with areas of increased Coulomb stress changes following the mainshock. The majority of seismicity concentrated near the ruptured plane where the stress changes are in the positive values. Besides, the middle part of the high Zagros fault (HZF) and the northern part of the main recent fault (MRF) and Zagros foredeep fault (ZFF) received positive stress changes and are the probable place for the future large events.

Acknowledgments

We are thankful to International Institute of Earthquake Engineering and Seismology for supporting this research work in the framework of the project entitled "Application of short term seismic hazard analysis in Iran and proposing a new method based on combined statistical and physical approaches", and Iranian Seismological Center (IRSC) for providing aftershocks data. Finally, we are very grateful to two anonymous reviewers for their insightful and constructive comments, which significantly improved the manuscript.

References

1. Vernant, P., Nilforoushan, F., Hatzfeld, D., Abbassi, M.R., Vigny, C., Masson, F., Nankali, H., Martinod, J., Ashtiani, A., Bayer, R., and Tavakoli, F. (2004) Present-day crustal deformation and plate kinematics in the Middle East constrained by GPS measurements in Iran and northern Oman. *Geophysical Journal International*, **157**(1), 381-398.

2. Toda, S., Lin, J., and Stein, R.S. (2011) Using the 2011 M=9.0 Tohoku earthquake to test the Coulomb stress triggering hypothesis and to calculate faults brought closer to failure. *Earth, Planets and Space*, **63**, 725-730.

3. Parsons, T., Stein, R.S., Simpson, R.W., and Reasenberg, P.A. (1999) Stress sensitivity of fault seismicity: A comparison between limited-offset oblique and major strike-slip faults. *Journal of Geophysical Research: Solid Earth*, **104**(B9), 20183-20202.

4. Sumy, D.F., Cochran, E.S., Keranen, K.M., Wei, M., and Abers, G.A. (2014) Observations of static Coulomb stress triggering of the November 2011 M5.7 Oklahoma earthquake sequence. *Journal of Geophysical Research: Solid Earth*, **119**(3), 1904-1923.

5. Steacy, S., Jiménez, A., and Holden, C. (2013) Stress triggering and the Canterbury earthquake sequence. *Geophysical Journal International*, **196**(1), 473-480.

6. Reasenberg, P.A. and Simpson, R.W. (1992) Response of regional seismicity to the static stress change produced by the Loma Prieta earthquake. *Science*, **255**(5052), 1687-1690.

7. Ma, K.F., Chan, C.H., and Stein, R.S. (2005) Response of seismicity to Coulomb stress triggers and shadows of the 1999 Mw = 7.6 Chi-Chi, Taiwan, earthquake. *Journal of Geophysical Research: Solid Earth*, **110**(B5).

8. King, G.C., Stein, R.S., and Lin, J. (1994) Static stress changes and the triggering of earthquakes. *Bulletin of the Seismological Society of America*, **84**(3), 935-953.

9. Walker, R.T., Andalibi, M.J., Gheitanchi, M.R., Jackson, J.A., Karegar, S., and Priestley, K. (2005) Seismological and field observations from the 1990 November 6 Furg (Hormozgan) earthquake: a rare case of surface rupture in the Zagros Mountains of Iran. *Geophysical Journal International*, **163**(2), 567-579.

10. Madanipour, S., Ehlers, T.A., Yassaghi, A., Rezaeian, M., Enkelmann, E., and Bahroudi, A. (2013) Synchronous deformation on orogenic plateau margins: Insights from the Arabia-Eurasia collision. *Tectonophysics*, **608**, 440-451.

11. Motaghi, K., Shabanian, E., and Kalvandi, F. (2017) Underplating along the northern portion of the Zagros suture zone, Iran. *Geophysical Journal International*, **210**(1), 375-389.

12. Talebian, M. and Jackson, J. (2004) A reappraisal of earthquake focal mechanisms and active shortening in the Zagros mountains of Iran. *Geophysical Journal International*, **156**(3),

506-526.

13. Solaymani Azad, S., Saboor, N., Moradi, M., Ajhdari, A., Youssefi, T., Mashal, M., and Roustaie, M. (2017) *Preliminary Report on Geological Features of the Ezgaleh-Kermanshah Earthquake (M~7.3), November 12, 2017, West Iran*. SSD of GSI Preliminary Report Number: 17-01, ver.01

14. Hessami, K., Jamali, F., and Tabasi, H. (2003) *Major Active Faults Map of Iran, Scale 1:2500000*. International Institute of Earthquake Engineering and Seismology.

15. Scholz, C.H. (2002) *The Mechanics of Earthquakes and Faulting*. Cambridge University Press.

16. Stein, R.S. (1999) The role of stress transfer in earthquake occurrence. *Nature*, **402**(6762), p. 605.

17. Steacy, S., Marsan, D., Nalbant, S.S., and McCloskey, J. (2004) Sensitivity of static stress calculations to the earthquake slip distribution. *Journal of Geophysical Research: Solid Earth*, **109**(B4).

18. Steacy, S., Gomberg, J., and Cocco, M. (2005) Introduction to special section: Stress transfer, earthquake triggering, and time-dependent seismic hazard. *Journal of Geophysical Research: Solid Earth*, **110**(B5).

19. Zarifi, Z., Nilfouroushan, F., and Raeesi, M. (2014) Crustal stress map of Iran: insight from seismic and geodetic computations. *Pure and Applied Geophysics*, **171**(7), 1219-1236.